NASA Contractor Report 199883

Effects of Spatial Gradients on Electron Runaway Acceleration

P. MacNeice and N. N. Ljepojevic

CONTRACT NAS5-32350
AUGUST 1996

NASA Contractor Report 199883

Effects of Spatial Gradients on Electron Runaway Acceleration

P. MacNeice
Hughes STX
Greenbelt, Maryland

N. N. Ljepojevic
Centre for Computer and Mathematical Modelling
South Bank University
London, SE1 0AA, UK

Prepared for
Goddard Space Flight Center
under Contract NAS5-32350

National Aeronautics
and Space Administration

Scientific and Technical
Information Branch

1996

This publication is available from the NASA Center for AeroSpace Information,
800 Elkridge Landing Road, Linthicum Heights, MD 21090-2934, (301) 621-0390.

Effects of Spatial gradients on Electron Runaway Acceleration

P. MacNeice
Hughes STX, Goddard Space Flight Center
Greenbelt, MD 20771
peter.macneice@gsfc.nasa.gov
and
N.N.Ljepojevic
Centre for Computer and Mathematical Modelling
South Bank University
London SE1 0AA, UK
ljepojnn@sbu.ac.uk

June 14, 1996

Abstract

The runaway process is known to accelerate electrons in many laboratory plasmas and has been suggested as an acceleration mechanism in some astrophysical plasmas, including solar flares. Current calculations of the electron velocity distributions resulting from the runaway process are greatly restricted because they impose spatial homogeneity on the distribution. We have computed runaway distributions which include consistent development of spatial gradients in the energetic tail. Our solution for the electron velocity distribution is presented as a function of distance along a finite length acceleration region, and is compared with the equivalent distribution for the infinitely long homogeneous system (ie. no spatial gradients), as considered in the existing literature. All these results are for the weak field regime. We also discuss the severe restrictiveness of this weak field assumption.

1 INTRODUCTION

When a DC electric field is applied to a plasma runaway acceleration occurs of electrons above a critical velocity. This process is a consequence of the decrease of the dynamical friction [3] experienced by an electron when its speed increases above ion thermal speeds.

This process is known to be important in laboratory plasmas such as tokomaks and other toroidal discharge devices [14], as well as in astrophysical plasmas eg solar flares. To date however, calculations of the velocity distribution and production rate of runaway electrons have been limited to the unphysical ideal of an homogeneous plasma of infinite spatial extent. This idealisation, though not strictly correct in tokomak plasmas, is rescued to an extent by the tokomaks toroidal periodicity. However in astrophysical contexts it is obviously inappropriate.

In reality runaway acceleration occurs in finite sized acceleration regions which may also be inhomogeneous. These spatial gradients can significantly affect the development of the runaway process. In this paper we investigate the role of spatial gradients on the runaway process. In particular we consider how spatial gradients can develop in the tail of the distribution due to the finite size of the acceleration region.

Our calculations have been made subject to the conventional assumption of a weak electric field. We reconsider the implications of this weak field assumption which is in our opinion significantly more restrictive than has been recognised in much of the existing literature.

In section 2 we briefly review the existing calculations of runaway rate and velocity distribution. The theory and numerical technique behind our calculation of the electron velocity distribution is discussed in section 3. In section 4 we present our results and compare them with existing calculations which ignore the spatial variation.

2 THEORY

Previous attempts to understand the runaway process can be divided into two broad categories. The Langevin approach considers the trajectories of test particles moving through an unchanging background plasma. The second approach is to establish and solve an appropriate equation describing the electron velocity distribution. This second approach is clearly superior in principle. However it has proven so difficult in practice that it has only been

accomplished under the restrictive assumption that the plasma is infinite and homogeneous in space.

The essence of the electron runaway process is most easily seen using the Langevin formulation. Consider an electron test particle moving through a background plasma in the presence of an externally applied DC electric field. The test electron is accelerated by the field. However it also experiences an effective frictional deceleration in the direction of its motion relative to the plasma. This is due to its many Coulomb interactions with the surrounding plasma particles. This frictional drag is greatest for an electron with velocity close to the thermal velocity of the local ion population [14]. Above the ion thermal velocity the frictional drag is a decreasing function of electron velocity. Thus there is always some velocity above which the electric field acceleration is greater than the frictional deceleration. Once above this critical velocity the effective acceleration of the electron grows as its velocity grows. This is the essence of runaway acceleration.

The Langevin formulation is physically intuitive but incomplete. It neglects the diffusion in speed and pitch angle experienced by the test particle. It also lacks consistency since the background plasma can be considered as a collection of test particles and so should also evolve under the influence of the applied field.

The electric field required to cause runaway behaviour for a thermal electron ($v_{th}^2 = 2kT_e/m_e$) is known as the Dreicer field, E_D. The importance of the runaway process in the overall force balance of the plasma can then be gauged by comparing the electric field to the Dreicer field. Calculations of electron distributions resulting from runaway have always been restricted to the weak field regime $E/E_D < 0.1$. We also assume this restriction. This implies that only an exponentially small fraction of electrons will run away, admitting the possibility that the bulk of the distribution can remain close to maxwellian and near steady state. The ratio of electric field to Dreicer field is often rewritten as $(v_{th}/v_{cr})^2$, where the critical speed v_{cr} is the speed at which acceleration by the electric field and frictional drag balance exactly.

Many different estimates of the rate of production of runaway electrons in this weak field regime exist in the literature. The earliest were presented by Giovanelli [11] and Harrison [12]. However Dreicer [5, 6] is generally credited with the first detailed analysis. He considered the abrupt application of a weak uniform electric field to an infinite homogeneous and ionized plasma. His runaway rate was determined from the rate of decay of the total population of collisional electrons below the critical speed. He did not determine the form of the distribution in the runaway regime. His solution was also

compromised by his assumption that the distribution function dropped to zero on the sphere of radius v_c in velocity space.

Both Gurevich [9] and Lebedev [17] attempted analytic solutions to the same problem by assuming a quasi-stationary distribution (ie. $\partial/\partial t \sim 0$) and applying different functional approximations for the electron velocity distribution function f over different regions of velocity space. Kruskal and Bernstein [15] and Gurevich and Zhivlyuk [10] developed this approach most fully. By identifying five seperate regions of velocity space Kruskal and Bernstein determined a runaway rate to within an unknown constant multiplying factor. Since then a number of numerical solutions of this problem have been published [16, 22, 7]. By comparing their numerical determination of the runaway rate to that of Kruskal and Bernstein, Kulsrud et al determined this unknown numerical multiplying factor. The resulting runaway rate,

$$\lambda = 0.35 n_e \nu (v_{th}/\sqrt{2}) \left(\frac{E}{2E_D}\right)^{-3/8} exp\left(-\left(\frac{4E_D}{E}\right)^{1/2} - \frac{E_D}{2E}\right).$$

is the most frequently quoted runaway rate in the literature. Here ν is the electron collision frequency and n_e the electron number density.

In the interest of clarity we point out that a critical electric field E_{cr} is often defined which is the field required to balance the drag experienced by an electron with speed kT_e/m_e. The critical and Dreicer fields are related by $E_{cr} = 2E_D = 4\pi e^3 n_e \ln\Lambda / kT_e$.

3 APPROXIMATING THE ELECTRON DISTRIBUTION FUNCTION

Our method of approximating the electron distribution function is described in greater detail in Ljepojevic and Burgess [18] and Ljepojevic and MacNeice [19]. The electron distribution function in a plasma can be found by solving the Boltzmann transport equation

$$\frac{\partial f}{\partial t} + \boldsymbol{v} \cdot \frac{\partial f}{\partial \boldsymbol{x}} + \frac{\boldsymbol{F}}{m_e} \cdot \frac{\partial f}{\partial \boldsymbol{v}} = \left(\frac{\partial f}{\partial t}\right)_c \tag{1}$$

where f is the electron distribution function, $\boldsymbol{v}$ is the electron velocity, $\boldsymbol{x}$ is the position vector, $\boldsymbol{F}$ includes all forces acting on the electrons, and the right hand-side of the equation describes the rate of change of f as a result of collisional redistribution of electrons in velocity space. It is generally true

that the terms on the left hand-side of equation (1) represent effects driving the plasma away from Maxwellian, while the right hand-side describes thermalising collisional redistribution.

Rosenbluth, MacDonald and Judd [20] have shown that when only 2-body Coulomb collisions need be considered, and $v^2/c^2 \ll 1$,

$$\left(\frac{\partial f}{\partial t}\right)_c = -\Gamma \frac{\partial}{\partial v^\mu}\left(f \frac{\partial H}{\partial v^\mu}\right) + \frac{1}{2}\frac{\partial^2}{\partial v^\mu \partial v^\nu}\left(f \frac{\partial^2}{\partial v^\mu \partial v^\nu} G\right), \tag{2}$$

with

$$H(\boldsymbol{v}) = \sum_b \frac{m_e + m_b}{m_b} \int d^3v' \; f_b(\boldsymbol{v}') \mid \boldsymbol{v} - \boldsymbol{v}' \mid^{-1},$$

$$G(\boldsymbol{v}) = \sum_b \int d^3v' \; f_b(\boldsymbol{v}') \mid \boldsymbol{v} - \boldsymbol{v}' \mid,$$

and

$$\Gamma = \frac{4\pi e^4 \ln\Lambda}{m_e^2}.$$

$\ln\Lambda$ is the Coulomb logarithm, b denotes the particle species in the plasma (including other electrons) with which the electrons collide and c is the speed of light.

Equation (1) with equation (2) is non-linear. In the low and high velocity regimes it admits linearisation, the Spitzer-Härm/Braginskii(SH) approximation at low velocities, and the high velocity Landau(HVL) approximation at high velocities. Our solution is constructed by combining these approximations as described below.

For reasons of simplicity we assume that the plasma is fully ionized hydrogen in steady-state. The system boundaries are two parallel planes separated by a distance L. Electrons entering this system across these boundaries are assumed to have a Maxwellian velocity distribution. A uniform electic field is applied between these two parallel planes in the direction perpendicular to the planes. This idealised plasma therefore will exhibit spatial variation only in the direction of the electric field. We shall associate a cartesian coordinate s with this direction. We also assume that this applied electric field is sufficiently weak that the lower velocity bulk of the distribution is adequately described by the SH approximation. Finally we assume that there is no spatial variation in the bulk of the distribution.

3.1 The Spitzer-Härm/Braginskii approximation

This approach is based on Enskog's successive approximation (cf. Chapman and Cowling [4]). It proceeds under the assumptions that the distribution function exhibits slow temporal variation and weak spatial gradients, and is subject to weak electromagnetic fields. As a result the distribution function can be written as

$$f = f_0 + f_1 + f_2 + \cdots,$$

where successive terms represent increasingly smaller corrections. The zeroth order term f_0 is taken to be a Maxwellian. This approximation is similar to a perturbation expansion in a small parameter although no small parameter has been explicitly designated. In fact we shall see that the solution behaves as though the Knudsen parameter were that small parameter.

Spitzer and Härm [21] considered a plasma with a weak temperature gradient and coaligned electric field (here assumed along the s axis). They adopted a first order scheme which requires

$$f_1 = f_0 D(v)\mu,$$

where $\mu = \mathrm{Cos}\theta = \boldsymbol{v} \cdot \hat{s}/v = \cos\theta$ is the cosine of the electron pitch angle. D is a function of the electron speed determined by substituting for f in the Boltzmann equation, linearising the collisional integral in f_1, and solving the resulting integro-differential equation. The solution has the form

$$f = f_0 \left\{ 1 - \lambda_0 \left[\frac{ZD_E}{A} \left(\frac{eE}{kT_e} + \frac{1}{p_e} \frac{\partial p_e}{\partial s} \right) - 2 \frac{ZD_T}{B} \frac{1}{T_e} \frac{\partial T_e}{\partial s} \right] \mu \right\},$$

where ZD_E/A and ZD_T/B are tabulated in SH, p_e is the electron pressure, T_e is the electron temperature, E the electric field, A and B are normalisation constants for the electric field and temperature gradient respectively, and λ_0 is the mean free path of a thermal electron. D_E and D_T increase with velocity and for $\mu > 0$ a speed $v^*(\mu)$ exists above which f becomes negative. It is also clear that as the scale lengths $(\partial \ln T_e/\partial s)^{-1}$, $(\partial \ln p_e/\partial s)^{-1}$ and kT_e/eE decrease, $v^*(\mu)$ decreases. Thus the Spitzer-Härm approach is only valid in the low velocity regime, and the upper boundary of this regime depends on the strength of the electric field and temperature and pressure gradients (see Gray and Kilkenny [8]). As mentioned earlier, in this paper we assume $\partial T_e/\partial s = \partial p_e/\partial s = 0$.

3.2 High velocity — the HVL approximation

If we neglect the interaction between the high energy tail electrons in comparison with their coupling to the bulk of the distribution which is close to Maxwellian, then we can derive an approximate linearised form of equation (1), applicable to the high velocity electrons. Together with the assumptions that the plasma is inhomogeneous in the direction of the s axis only, and in steady state, equation (1) then becomes [18]

$$v\mu\frac{\partial f}{\partial s} - \frac{e\boldsymbol{E}}{m_e}\cdot\frac{\partial f}{\partial \boldsymbol{v}} = \frac{1}{v^2}\frac{\partial}{\partial v}\left[v^2\nu(v)\left(\frac{kT_e}{m_e}\frac{\partial f}{\partial v} + vf\right)\right] - \nu(v)\frac{\partial}{\partial \mu}\left[(1-\mu^2)\frac{\partial f}{\partial \mu}\right], \tag{3}$$

where

$$\nu(v) = \frac{4\pi e^4 n_e \ln\Lambda}{m_e^2 v^3},$$

with T_e being the temperature characterising the bulk of the electron distribution at height s and n_e the electron number density.

Equation (3) can then be applied to determine the velocity distribution of electrons at higher energies, above some appropriately chosen cutoff velocity v_c.

Our solution is constructed by combining the Spitzer-Härm solution below $\xi_c = v_c/v_{th}$ with the HVL solution above ξ_c. By experimenting with different values $\xi_c = 2$ has been found to be the optimal value. At ξ_c we require that the HVL solution match the SH solution for all pitch angles.

By choosing to extend the application of the Spitzer-Härm solution out to $\xi = 2$, we have placed an upper limit on the strength of the electric field which we can consider. We will choose to set $E/E_D = 0.05$. At this field strength the Spitzer-Härm distribution becomes negative for $\theta = \pi$ and ξ in excess of about 2.2. At higher field strengths the Spitzer-Härm distribution becomes negative at even lower speeds.

Equation (3) is a linearised form of the non-relativistic Landau equation. Obviously when the electron velocity becomes a significant fraction of the speed of light relativistic effects become important and equation (3) becomes invalid. An appropriate relativistic generalisation of the Landau equation has been derived [1, 13]. However it is considerably more complex in form, and for reasons of simplicity we have chosen to retain the non-relativistic form for this present work. This clearly limits the maximum temperatures of the bulk distributions which we can consider.

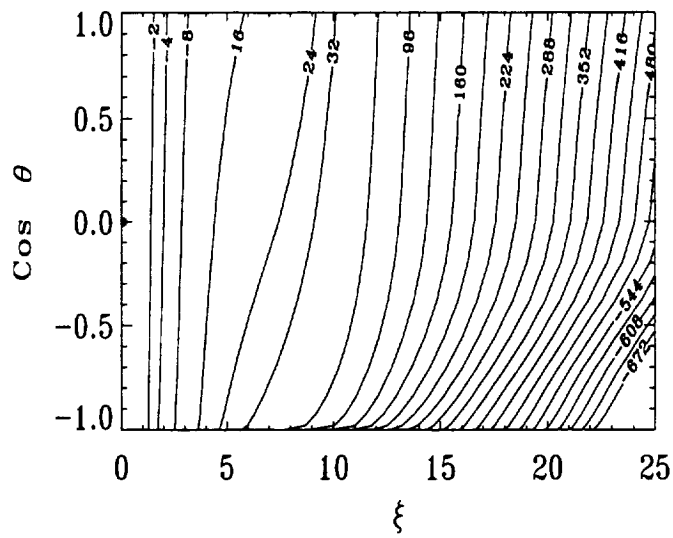

Figure 1: $\ln(f/f_N)$ variation with speed ξ and pitch angle θ at $s = 4.375 \times 10^9$cm, for $0 \leq \theta \leq \pi$ and $0 \leq \xi \leq 25$. Unlabelled contours are evenly spaced between labelled contours.

4 RESULTS

Equation (3) was solved for a plasma with bulk temperature 10^6K and electron number density 10^9cm^{-3}. A uniform electric field $\boldsymbol{E} = -0.05E_D\hat{s}$ was applied between the plane parallel system boundaries separated by a distance $L = 5 \times 10^9$cm. The solution was obtained for electron speeds up to $\xi = 25$ on a finite difference mesh with 80 grid cells along the s axis. The mean free path of a thermal electron in this plasma is approximately 8×10^6cm, or approximately one tenth of the spatial grid cell size. Since the electron mean free path scales as ξ^4, there are roughly two grid cells per mean free path at $\xi = 2$. The normalised critical velocity is $\xi_{cr} = v_{cr}/v_{th} = (E_D/E)^{1/2} \sim 4.5$.

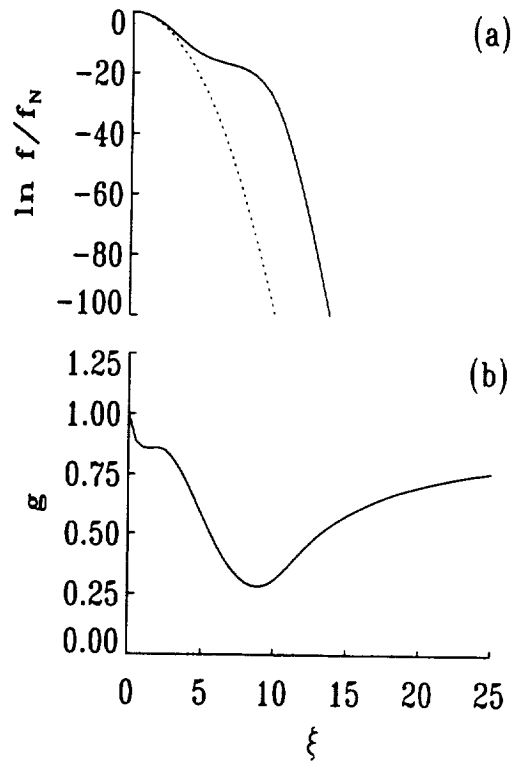

Figure 2: (a) Variation of $\ln(f/f_N)$ with speed ξ for pitch angle $\theta = 0$, ie. in the direction of electron acceleration, at $s = 4.375 \times 10^9$cm. The dashed curve is the equivalent maxwellian curve.(b) The same data plotted in (a) recast in the form of the exponent function g.

4.1 The Distribution Function

A convenient representation of the solution can be achieved by defining a function $g(s, \xi, \mu)$ such that

$$f = f_N \exp\left(-g\xi^2\right)$$

where the normalisation constant $f_N = n(2\pi kT_e/m_e)^{-3/2}$. A value of $g = 1$ gives the maxwellian value for f, $g > 1$ underpopulation relative to a maxwellian and $g < 1$ overpopulation relative to a maxwellian.

Figure 1 illustrates the structure in velocity space of our solution at a selected location, $s = 4.375 \times 10^9$cm. The tail of the distribution is overpopulated relative to a Maxwellian distribution for $\theta < \pi/2$. The variation

of both $\ln(f/f_N)$ and g with ξ for $\theta = 0$, ie the direction anti-parallel to the applied field, is shown in figures 2 a and b. At low velocity and very high velocity the distribution is close to maxwellian with temperature equal to the assumed bulk temperature. The distribution begins to depart significantly from maxwellian near $\xi \sim 3.5$ as the increasingly collisionless character of the electrons permits them to gain more energy from the applied field between collisions. The $\ln(f/f_N)$ curve "flattens" out somewhat before eventually turning down again to rejoin the original maxwellian curve at very high velocities. The extent of this "flattened" section of the curve is limited by the finite spatial extent of the acceleration region. As the length of the acceleration region is extended this flattened section is also extended (figure 3) and would ultimately extend to infinite velocities in the idealised case of an infinitely long acceleration region.

The typical variation of $\ln f$ with θ in the tail is illustrated in figure 4. Note that the distribution is enhanced above maxwellian in the direction perpendicular to the field. This is a consequence of the diffusive spread in pitch angle of the runaway tail.

In figure 5 we have plotted the variation of $\ln f$ with perpendicular speed $\xi_\perp$ at $s = 4.375 \times 10^9$cm for two different values of $\xi_\parallel = \boldsymbol{\xi} \cdot \hat{s}$ of 6 and 10. For $\xi_\perp \leq 5$ where most of the energy resides, this is well fit by a gaussian with a temperature of 1.6×10^6K, as indicated by the superimposed dashed line in figure 5b. Broadenning of this perpendicular velocity distribution persists at larger $\xi_\perp$ but with steadily diminishing degree, until for $\xi_\perp \geq 20$ the perpendicular distribution becomes Maxwellian at about the original background temperature of 10^6K. To determine the energy content of the perpendicular velocity distribution we define a perpendicular temperature

$$T_\perp(\xi_\parallel, s) = \int_0^\infty d\xi_\perp \xi_\perp^3 f(\xi_\parallel, \xi_\perp, s) \Big/ \int_0^\infty d\xi_\perp \xi_\perp f(\xi_\parallel, \xi_\perp, s)$$

following Fuchs et al [7]. This is plotted in figure 6 as a function of $\xi_\parallel$ at a number of different spatial locations throughout the acceleration region. For example at $s = 4.375 \times 10^9$cm and $\xi_\parallel = 10$ the perpendicular temperature is 1.6×10^6K as we would expect given the fit shown in figure 5b.

Obviously, in the absence of any explicit source of electrical current there should be no spatial variation of the total current. In our solution however the spatial variation of f above $\xi = 2$ represents a small variation in current. In reality any variation of this kind in the current would produce a local accumulation of charge resulting in a local electric field acting to disperse this accumulation. Therefore, in applying a fixed potential between the

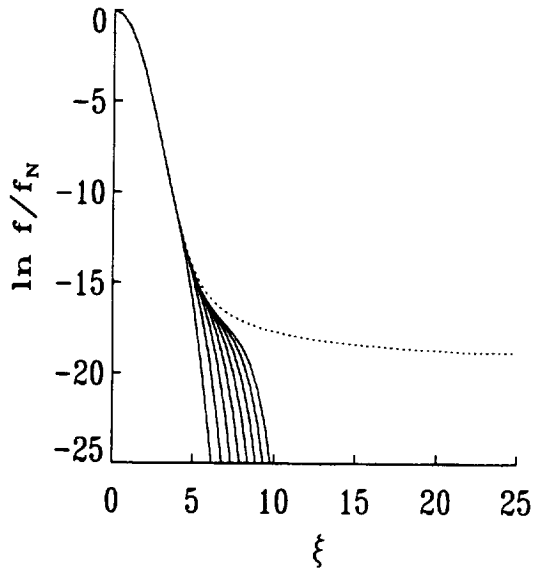

Figure 3: Variation of $\ln(f/f_N)$ with speed ξ for pitch angle $\theta = 0$ beginning at $s = 0$cm (leftmost solid curve), and continuing at regular intervals of 6.25×10^8cm up to 4.375×10^9cm (rightmost solid curve). The dotted line is for the infinitely long homogeneous case.

boundaries of the system we have not guaranteed that a uniform field will exist across the system. However in practice these departures from constant current which we observe are so slight that the local fields which should develop to restore current conservation can be neglected in comparison with the much larger applied field. The variation of the current density with position is illustrated in table 1.

The current flowing at $s_0 = 0$ is -3.364×10^7statamps cm^{-2}, while the current at $s = 5 \times 10^9$cm is -3.436×10^7statamps cm^{-2}. Most of the current is carred by the electrons below $\xi = 2$ which contribute -2.514×10^7statamps cm^{-2} to the total current density. This enables us to use the Spitzer-Härm electrical conductivity to calculate the approximate field cor-

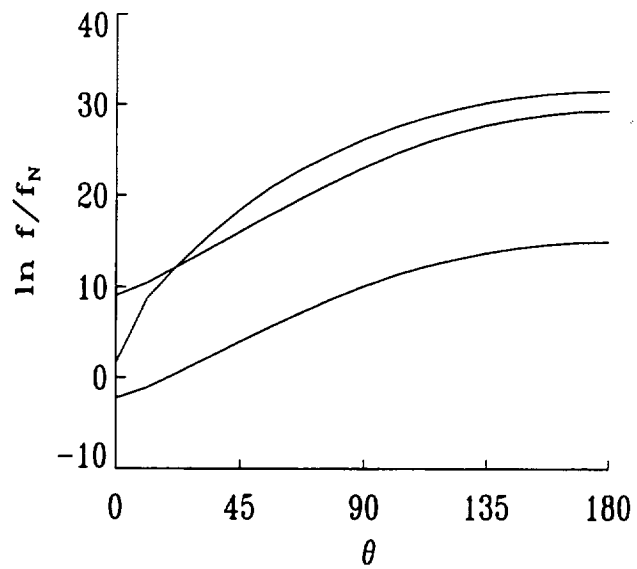

Figure 4: Variation of $\ln(f/f_N)$ with pitch angle θ for velocity $\xi = 7\hat{s}$ at $s = 6.25 \times 10^8$cm (lower curve), $s = 2.5 \times 10^9$cm and $s = 4.375 \times 10^9$cm (upper curve).

rection necessary to ensure constant current. In fact the ratio $\Delta E/E(s_0)$ should be approximately equal to $\Delta j/j(s_0) = 0.02$. This correction would have a negligible effect on the tail of the distribution.

What difference does inclusion of spatial gradients make to the velocity distribution? To answer this question we need to compare our results with the solution obtained when $\partial/\partial s = 0$, ie. the system is assumed infinite and homogeneous. As we have mentioned, such calculations have already been published [22, 16, 7]. Unfortunately these authors have always considered $E/E_D \geq 0.08$, and have applied the same linearised equation throughout all of velocity space with no special consideration of the thermal velocity regime. We have been limited to $E/E_D \leq 0.05$ precisely because of our application of the Spitzer-Härm distribution at thermal velocities. Therefore

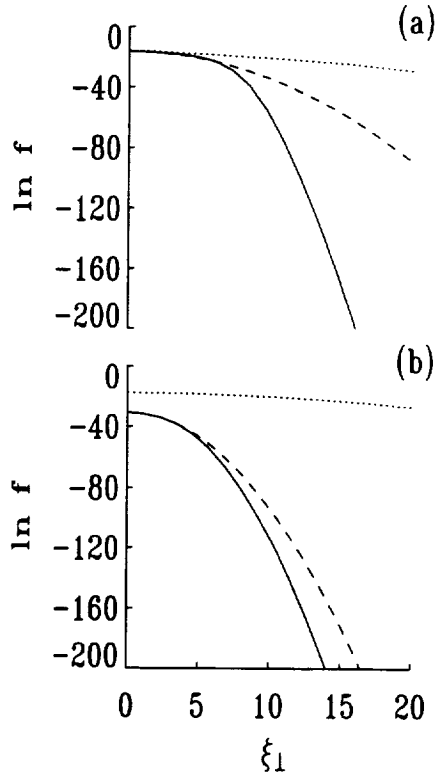

Figure 5: Distribution of perpendicular velocities of electrons at $s = 4.375 \times 10^9$cm (solid lines) with (a) $\xi_\parallel = \boldsymbol{\xi} \cdot \hat{s} = 6$ and (b) $\xi_\parallel = 10$. The dotted curves are the equivalent result for the infinite homogeneous case.

to isolate the differences introduced by consideration of spatial gradients it was necessary for us to generate a solution for the infinite homogeneous distribution with $E/E_D = 0.05$ and consistent with the application of the Spitzer-Härm distribution below $\xi = 2$. We used a relaxation approach similar to that of Wiley at al. [22]. The appropiate equation,

$$\frac{\partial f}{\partial t} - \frac{e\boldsymbol{E}}{m_e} \cdot \frac{\partial f}{\partial \boldsymbol{v}} = \frac{1}{v^2}\frac{\partial}{\partial v}\left[v^2 \nu(v)\left(\frac{kT_e}{m_e}\frac{\partial f}{\partial v} + vf\right)\right] - \nu(v)\frac{\partial}{\partial \mu}\left[(1-\mu^2)\frac{\partial f}{\partial \mu}\right], \tag{5}$$

was solved using a finite difference approximation until an almost steady state was achieved. This steady state distribution is illustrated in figures 3, 5 and 6. The infinite homogeneous solution appears to be the asymptotic limit to which the position dependent distribution tends as the length of the

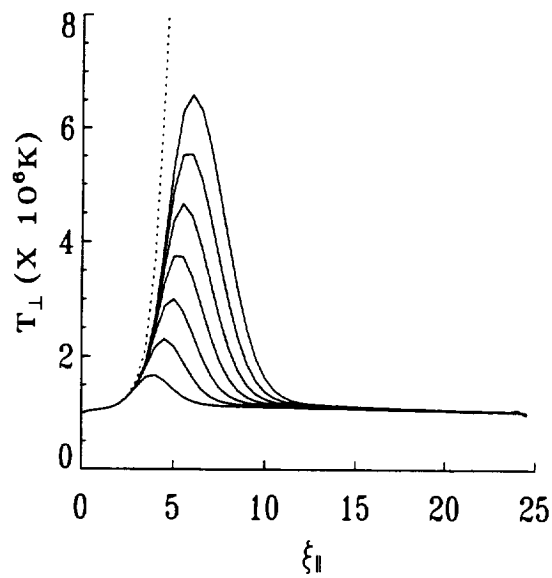

Figure 6: Variation of the perpendicular temperature $T_\perp$ with $\xi_\parallel$ and spatial location. Each curve represents a different spatial location beginning with the lowest solid curve at $s = 6.25 \times 10^8$cm, and continuing at regular intervals of 6.25×10^8cm out to the highest solid curve at $s = 4.375 \times 10^9$cm. The dotted curve is for the infinitely long homogeneous case.

acceleration region approaches infinity. The tail of this limit distribution, for $\theta = 0$, has an $f \propto 1/\xi$ dependence, as expected from conservation of flux arguments [2].

4.2 The Runaway Rate

How do these results compare with the runaway rates quoted in the literature? To compute runaway rates we have followed the example of Wiley et al [22]. Let us consider first the infinite homogeneous system. The rate of production of runaways can be computed from the rate of loss of electrons from the collisional bulk of the distribution. We choose to idealise the colli-

Table 1: Electric Current Density as a function of position for a uniform electric field $\boldsymbol{E} = -0.05E_D\hat{s}$.

s (10^9 cm)	j (10^7statamps.cm^{-2})
0.0000	3.364
0.1250	3.421
0.2500	3.422
0.3750	3.417
0.5000	3.414
0.6250	3.413
0.7500	3.413
⋮	⋮
4.6250	3.413
4.7500	3.413
4.8750	3.416
5.0000	3.436

sional regime as a sphere in velocity of radius ξ_R. Integrating the equation (5) over the volume of the collisional regime gives

$$\frac{\partial n_C}{\partial t} = -\frac{\partial n_R}{\partial t} = \frac{8\pi^2 n e^4 \ln\Lambda}{m_e^2}\int_{-1}^{1} d\mu \left(\frac{E}{E_D}\xi_R^2 f(\xi_R)\mu + \frac{1}{2\xi_R}\frac{\partial f}{\partial \xi}\bigg|_R + f(\xi_R)\right) \tag{6}$$

where n_C is the number of electrons in the bulk and n_R is the number of runaway electrons. For comparative purposes we define a normalised time

$$\tau = t\frac{4\pi e^4 \ln\Lambda}{m_e^2}\frac{1}{\pi\sqrt{\pi}}.$$

The runaway rate $\Gamma = n^{-1}\partial n_R/\partial\tau$ can be easily calculated once we have chosen an appropriate value for ξ_R. The obvious choice would seem to be the critical velocity $\xi_R = \xi_{cr}$. The variation of Γ with ξ_R is illustrated in figure 7. For the infinite homogeneous system, the rate decreases rapidly with increasing ξ_R until just above the critical velocity, near 4.5 in this case. It maintains a fairly constant value thereafter. This constant rate, which

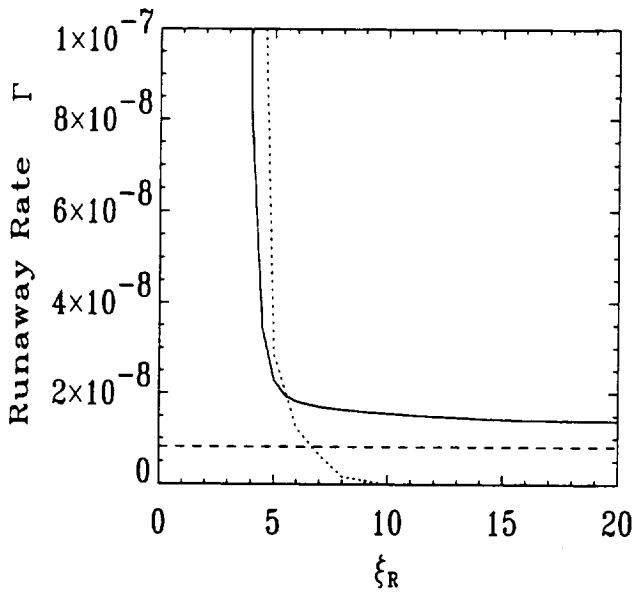

Figure 7: Variation of the rate Γ as a function of ξ_R for the case of the infinitely long homogeneous plasma(dotted line), and for position $s = 4.375 \times 10^9$cm along the finite sized acceleration region(solid line). The horizontal broken line indicates the runaway rate computed from the expression of Kruskal and Bernstein given in section 2.

is approximately 70% larger than predicted by the normalised Kruskal and Bernstein [15] formula is the obvious choice for the runaway rate.

When spatial gradients are retained in the calculation of the distribution function the identification of a runaway rate is much less clear. The integral of equation (3) over the collisional sphere in velocity space produces an equation identical to equation (6) except for the addition of a term due to the spatial gradient. However the spatial gradient term is responsible for convective transport of electrons, and does not result in any change to their speed. It does not contribute directly to the rate of production of runaways. Thus equation (6) can be used to compute the runaway rate in the presence

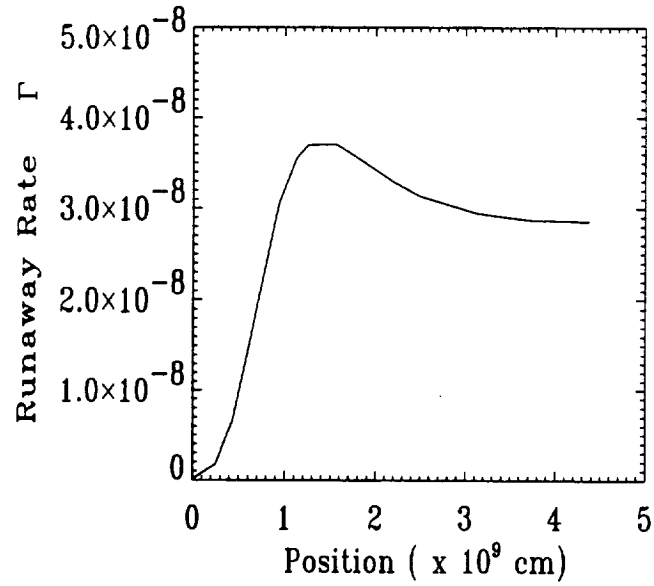

Figure 8: Variation of the runaway rate with position in the finite length acceleration region. The rate is computed using $\xi_R = 5$.

of spatial gradients also. In figure 7 we show the variation of Γ with ξ_R at $s = 4.375 \times 10^9$cm. As ξ_R increases the rate drops steadily. The energetic tail has not developed sufficiently to produce a rate independent of ξ_R as was the case in the infinite homogeneous system. The runaway rate is clearly sensitively dependent on our choice of ξ_R. We will choose $\xi_R = 5$ for two reasons. The first is that it lies just above the critical runaway velocity $\xi_{cr} = 4.5$ which is where the rate became insensitive to the value of ξ_R in the infinite homogeneous case. The second is that this is the same choice adopted by Wiley et al [22]. In figure 8 we show how this runaway rate varies as a function of position along the acceleration region.

5 DISCUSSION

This present calculation is limited in the maximum values of E/E_D and T_e which can be considered. Our requirement to match solutions above and below $\xi = 2$ limits the size of the electric field . For $E/E_D > .05$ the Spitzer-Härm solution is no longer sufficiently accurate near $\xi = 2$. This limitation can only be overcome by more accurately solving the non-linear equation which defines the distribution function in the region of the thermal velocity. No other numerical calculations of the runaway rate have addressed this difficulty satisfactorily in spite of the fact that they typically apply electric fields in the range $0.08 \leq E/E_D \leq 0.2$. The limitation on the bulk temperatures which we can consider is a consequence of our non-relativistic treatment. By raising the temperature we push the runaway regime to a higher range in $(v/c)^2$.

Our results show that except during the initial stages of acceleration the runaway rate predicted by the normalised Kruskal and Bernstein theory is accurate to within a factor of two. However in any application which requires the actual distribution of electrons rather than the total number in the tail, the infinite homogeneous result is capable of being in error by orders of magnitude.

6 ACKNOWLEDGMENTS

This research was sponsored in part by NASA HQ Solar Physics Office Grant number 170–38–53–21. We wish to thank Drs. Spicer, Holman and Benka for their critical comments.

References

[1] Beliaev S.T. and Budker G.I., *Soviet Phys. Doklady*, **1**, 218, (1956).

[2] *private communication*, (1991).

[3] Chandrasekhar S., *Ap.J.*, **97**, 255, (1943).

[4] Chapman S. and Cowling T.G., *The Mathematical Theory of Non-Uniform Gases*, (Cambridge University Press), Chapter 7, (1970).

[5] Dreicer H., *Phys.Rev.*, **115**, 238, (1959).

[6] Dreicer H., *Phys.Rev.*, **117**, 329, (1960).

[7] Fuchs V., Cairns R.A. and Lashmore-Davies C.N., *Phys.Fluids*, **29**, 2931, (1986).

[8] Gray D.R. and Kilkenny J.D., *Plasma Phys.*, **22**, 81, (1980).

[9] Gurevich A.V., *Sov. Phys. JETP*, **12**, 904, (1961).

[10] Gurevich A.V. and Zhivlyuk Yu.N., *Sov. Phys. JETP*, **22**, 153, (1966).

[11] Giovanelli R.G., *Phil.Mag.(Seventh Series)*, **40**, 206, (1949).

[12] Harrison E.R., *Phil.Mag.(Eight Series)*, **3**, 1318, (1958).

[13] Klimontovich Yu.L., *Kinetic Theory of Nonideal Gases and Nonideal Plasmas*, (Pergamon Press), Chapter 7,(1982).

[14] Knoepfel H. and Spong D.A., *Nuclear Fusion*, **19**, 785, (1979).

[15] Kruskal M. and Bernstein I.B., *Princeton Plasma Physics Lab. Report*, Matt–Q–20, 174, (1962).

[16] Kulsrud R.M., Sun Y-C., Winsor N.K. and Fallon H.A, *Phys. Rev. Letts.*, **31**, 690, (1973).

[17] Lebedev A.N., *Sov. Phys. JETP*, **21**, 931, (1965).

[18] Ljepojevic N.N. and Burgess A., *Proc. Roy. Soc. London A*, **428**, 71, (1990).

[19] Ljepojevic N.N. and MacNeice P., *Sol. Phys.*, **117**, 123, (1988).

[20] Rosenbluth M.N., MacDonald W. and Judd,D., *Phys.Rev.*, **107**, 1, (1957).

[21] Spitzer L. and Härm R., *Phys.Rev.*, **89**, 977, (1953).

[22] Wiley J.C., Choi D-I. and Horton W., *Phys. Fluids*, **23**, 2193, (1980).

REPORT DOCUMENTATION PAGE

Form Approved
OMB No. 0704-0188

Public reporting burden for this collection of information is estimated to average 1 hour per response, including the time for reviewing instructions, searching existing data sources, gathering and maintaining the data needed, and completing and reviewing the collection of information. Send comments regarding this burden estimate or any other aspect of this collection of information, including suggestions for reducing this burden, to Washington Headquarters Services, Directorate for Information Operations and Reports, 1215 Jefferson Davis Highway, Suite 1204, Arlington, VA 22202-4302, and to the Office of Management and Budget, Paperwork Reduction Project (0704-0188), Washington, DC 20503.

1. AGENCY USE ONLY *(Leave blank)*

2. REPORT DATE
August 1996

3. REPORT TYPE AND DATES COVERED
Contractor Report

4. TITLE AND SUBTITLE
Effects of Spatial Gradients on Electron Runaway Acceleration

5. FUNDING NUMBERS
Code 934

6. AUTHOR(S)
Peter MacNeice and N. N. Ljepojevic

7. PERFORMING ORGANIZATION NAME(S) AND ADDRESS(ES)
Hughes STX
4400 Forbes Boulevard
Lanham, Maryland 20706

8. PERFORMING ORGANIZATION REPORT NUMBER
96B00104

9. SPONSORING/MONITORING AGENCY NAME(S) AND ADDRESS(ES)
Goddard Space Flight Center
National Aeronautics and Space Administration
Washington , DC 20546-0001

10. SPONSORING/MONITORING AGENCY REPORT NUMBER
CR-199883

11. SUPPLEMENTARY NOTES
Peter MacNeice: Hughes STX, Lanham, Maryland
N. N. Ljepojevic: Centre for Computer and Mathematical Modelling, South Bank University, London, UK

12a. DISTRIBUTION/AVAILABILITY STATEMENT
Unclassified-Unlimited
Subject Catagory: 75
This report is available from the NASA Center for AeroSpace Information, 800 Elkridge Landing Road, Linthicum Heights, MD 21090; (301) 621-0390

12b. DISTRIBUTION CODE

13. ABSTRACT *(Maximum 200 words)*

The runaway process is known to accelerate electrons in many laboratory plasmas and has been suggested as an acceleration mechanism in some astrophysical plasmas, including solar flares. Current calculations of the electron velocity distributions resulting from the runaway process are greatly restricted because they impose spatial homogeneity on the distribution. We have computed runaway distributions which include consistent development of spatial gradients in the energetic tail. Our solution for the electron velocity distribution is presented as a function of distance along a finite length acceleration region, and is compared with the equivalent distribution for the infinitely long homogenous system (i.e., no spatial gradients), as considered in the existing literature. All these results are for the weak field regime. We also discuss the severe restrictiveness of this weak field assumption.

14. SUBJECT TERMS
Astrophysical plasma, electron, velocity, runaway, distribution, spatial gradients

15. NUMBER OF PAGES
19

16. PRICE CODE

17. SECURITY CLASSIFICATION OF REPORT	18. SECURITY CLASSIFICATION OF THIS PAGE	19. SECURITY CLASSIFICATION OF ABSTRACT	20. LIMITATION OF ABSTRACT
Unclassified	Unclassified	Unclassified	Unlimited

National Aeronautics and
Space Administration

Goddard Space Flight Center
Greenbelt, Maryland 20771

Official Business
Penalty for Private Use, $300

SPECIAL FOURTH-CLASS RATE
POSTAGE & FEES PAID
NASA
PERMIT No. G27

POSTMASTER: If Undeliverable (Section 158, Postal Manual) Do Not Return